Indian J. pure appl. Math., 27(8) : 821-835, August 1996

PROPAGATION OF MICROPOLAR WAVES AT BOUNDARY SURFACE

RAJNEESH KUMAR[1] AND S. K. TOMAR[2]

[1]*Department of Mathematics, Kurukshetra University, Kurukshetra* 132 119.
[2]*Department of Applied Mathematics, P. G. Regional Centre, Hisar*

(*Received* 22 *September* 1995; *accepted* 29 *January* 1996)

In the present work an attempt is made to study the behaviour of amplitude ratios of various reflected and refracted waves at a boundary surface. The following problems have been discussed : (i) the reflection and refraction of coupled transverse and micro-rational waves at an interface of liquid-micropolar half-space and elastic solid half-space; (ii) Reflection of coupled transverse and micro-rotational waves at a fixed boundary of a micropolar elastic half-space; and (iii) Reflection of longitudinal micro-rotational wave at a fixed boundary. The values of the modulus of amplitude ratios have been computed for particular models in all these three problems. The numerical results have been depicted graphically. A special case has been discussed.

INTRODUCTION

Theory of micropolar continua was proposed by Eringen and Suhubi[1] and Eringen[2] to describe the continuum behaviour of materials possessing micro-structure. Basically, the difference between classical continuum theories and that of micropolar continuum theory is that the later admits independent rotations of the material's substructure; that is, the local intrinsic rotations (micro-rotations) which are taken to be kinematically independent of the linear displacements. It is believed that such a theory is applicable in the treatment of granular and fibrous composite materials.

The granular nature of the material, microstructure, becomes important in transmitting waves of small wave length and/or high frequency because they may reveal new types of waves not encountered in the classical theory of elasticity. Even when the grain size is not visible to the eye if the wave length is comparable with the average grain size, the motion of the grains must be taken into account. In such cases, the local micromotion may in fact become dominant.

Parfitt and Eringen[5] have investigated the problem of reflection of plane waves from the flat boundary of a micropolar elastic half-space and obtained the expressions for amplitude ratio of different reflected waves in a closed form. The propagation of plane micropolar waves in an infinite medium have also been presented nicely.

Ariman[3] discussed the wave propagation in a micropolar elastic medium and the reflection of plane longitudinal displacement wave from a fixed flat surface of a micropolar elastic half-space. Reflection and refraction of a longitudinal micro-rotation wave at an interface between two micropolar elastic solids in welded contact has been investigated by Tomar and Gogna[6].

BASIC EQUATIONS

Following Eringen[2] the constitutive relations and the field equations for micropolar elastic solids in the absence of body force and body couple can be written as

$$\left.\begin{aligned} t_{kl} &= \lambda u_{r,\,r}\,\delta_{kl} + \mu(u_{k,\,l} + u_{l,\,k}) + K(u_{l,\,k} - \varepsilon_{klr}\,\phi_r), \\ m_{kl} &= \alpha\phi_{r,\,r}\,\delta_{kl} + \beta\phi_{k,\,l} + \gamma\,\phi_{l,\,k}, \end{aligned}\right\} \quad \ldots (1)$$

$$\left.\begin{aligned} (c_1^2 + c_3^2)\,\nabla(\nabla\cdot\vec{u}) - (c_2^2 + c_3^2)\,\nabla x\,(\nabla x\,\vec{u}) + c_3^2\,\nabla x\,\vec{\phi} &= \frac{\partial^2\vec{u}}{\partial t^2}, \\ (c_4^2 + c_5^2)\,\nabla(\nabla\cdot\vec{\phi}) - c_4^2\,\nabla x\,(\nabla x\,\vec{\phi}) + \omega_0^2\,\nabla x\,\vec{u} - 2\omega_0^2\,\vec{\phi} &= \frac{\partial^2\vec{\phi}}{\partial t^2}, \end{aligned}\right\} \quad \ldots (2)$$

where $c_1^2 = (\lambda + 2\mu)/\rho, \quad c_2^2 = \mu/\rho\ , \ c_3^2 = K/\rho,$

$$c_4^2 = \gamma/\rho j, \ c_5^2 = (\alpha + \beta)/\rho j, \ \omega_0^2 = K/\rho j$$

$\lambda, \mu, K, \alpha, \beta, \gamma$ are the material moduli, ρ the density of the medium, j the micro-inertia. $\vec{u}$ and $\vec{\phi}$ are displacement and micro-rotation vector respectively. Other symbols have their usual meanings.

By Helmholtz representation of vectors, we can write

$$\left.\begin{aligned} \vec{u} &= \nabla q + \nabla x\,\vec{U}, \quad \nabla\cdot\vec{U} = 0, \\ \vec{\phi} &= \nabla\xi + \nabla x\,\vec{\Phi}, \quad \nabla\cdot\vec{\Phi} = 0. \end{aligned}\right\} \quad \ldots (3)$$

Substituting eqns. (3) in eqns. (2), we obtain

$$(c_1^2 + c_3^2)\,\nabla^2 q = \frac{\partial^2 q}{\partial t^2}\ , \quad \ldots (4)$$

$$(c_4^2 + c_5^2)\,\nabla^2\xi - 2\omega_0^2\,\xi = \frac{\partial^2\xi}{\partial t^2}\ , \quad \ldots (5)$$

$$(c_2^2 + c_3^2)\,\nabla^2\vec{U} + c_3^2\,\nabla x\,\vec{\Phi} = \frac{\partial^2\vec{U}}{\partial t^2}\ , \quad \ldots (6)$$

$$b_1 = -\sin\theta_1 \cos\theta_1,\ b_2 = -1,\ b_3 = \sin\theta_1,\ b_4 = \cos\theta_4. \qquad \ldots (1.16)$$

The non-dimensional form of coefficients a_{ij} in eqn. (1.14) are as follows :

$$a_{11} = \frac{\lambda}{\mu} + F_1 (1 - V_r^2 \cos^2\theta_1)/F_1 V_r,$$

$$a_{12} = -\cos\theta_1 [1 - V_s^2 \cos^2\theta_1]^{1/2}/V_s ,$$

$$a_{13} = -\sin\theta_1 \cos\theta_1 ,$$

$$a_{14} = (\lambda'/\lambda)(\lambda/\mu)(V_4/\alpha')^2/F_1,$$

$$a_{21} = F_1 \cos\theta_1 [1 - V_r^2 \cos^2\theta_1]^{1/2} \left(\left[F_1 \sin^2\theta_1 - 1 + \frac{K}{\mu}\frac{1}{R_2} \right] V_r \right)^{-1} ,$$

$$a_{22} = \left(F_1 \sin^2\theta_3 - 1 + \frac{K}{\mu}\frac{1}{R_1} \right) \left(\left[F_1 \sin^2\theta_1 - 1 + \frac{K}{\mu}\frac{1}{R_2} \right] V_s^2 \right)^{-1}$$

$$a_{23} = 1,\ a_{24} = 0,\ a_{31} = 0,$$

$$a_{32} = R_2 [1 - V_s^2 \cos^2\theta_1]/R_1 V_s^3 ,\quad a_{33} = \sin\theta_1,\ a_{34} = 0,$$

$$a_{41} = [1 - V_r^2 \cos^2\theta_1]/V_r,\ a_{42} = -\cos\theta_1,$$

$$a_{43} = -\cos\theta_1,\ a_{44} = [1 - V_m^2 \cos^2\theta_1]^{1/2}/V_m , \qquad \ldots (1.17)$$

where

$$\left.\begin{aligned} &F_1 = (2 + K/\mu),\ V_r = V_1/V_4 , \\ &V_s = V_3/V_4 ,\ V_m = \alpha'/V_4 , \\ &R_1 = K_3^2 V_3^2/\omega_0^2 - 2 - K_3^2 c_4^2/\omega_0^2 , \\ &R_2 = K_4^2 V_4^2/\omega_0^2 - 2 - K_4^2 c_4^2/\omega_0^2 . \end{aligned}\right\} \qquad \ldots (1.18)$$

Special Case

If we let $\lambda' = 0$ then liquid half-space is not there and in this case the problem reduces to the problem of Parfitt and Eringen[5] of reflection of coupled waves at a flat free surface. It can be seen from the boundary conditions (1.10)-(1.11) that if we put $\lambda' = 0$ these boundary conditions and solving for reflection coefficients making use of same notations used by Parfitt and Eringen[5] we get the same reflection coefficients as obtained by these authors.

2. Reflection of Coupled Transverse and Micro-Rotation Waves From a Fixed Surface

In this case, we discuss the reflection of coupled transverse and microrotational waves at a fixed surface of a micropolar half-space. The geometry of the problem is shown in Fig. 2.

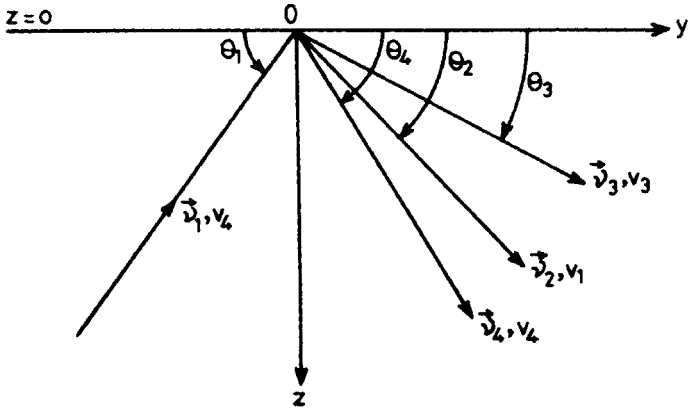

Fig. 2. Reflection of coupled wave.

At the plane boundary $z = 0$, the displacement components u_2 and u_3 and the micro-rotation ϕ_x must vanishes. Thus

$$\left.\begin{aligned} u_2 &= \frac{\partial q}{\partial y} + \frac{\partial U_x}{\partial z} = 0, \\ u_3 &= \frac{\partial q}{\partial z} - \frac{\partial U_x}{\partial y} = 0, \\ \phi_x &= \frac{\partial \Phi_z}{\partial y} - \frac{\partial \Phi_y}{\partial z} = 0 \end{aligned}\right\} \text{ at } z = 0. \qquad \ldots (2.1)$$

Substituting the values of potentials given by (1.1)-(1.5) in the boundary conditions (2.1) and using (1.8), (1.9), (1.12) and (1.13), we obtain

$$\left.\begin{aligned} &\frac{K_1}{K_4}(\sin\theta_2)\,Z_1 - \frac{K_3}{K_4}(\cos\theta_3)\,Z_2 - (\cos\theta_4)\,Z_3 = \cos\theta_1, \\ &\frac{K_1}{K_4}(\cos\theta_2)\,Z_1 + \frac{K_3}{K_4}(\sin\theta_3)\,Z_2 + \sin\theta_4\,Z_3 = \sin\theta_1, \\ &\left(\frac{K_3}{K_4}\right)^2 \frac{R_2}{R_1} Z_2 + Z_3 = -1 \end{aligned}\right\} \qquad \ldots (2.2)$$

where Z_1, Z_2 and Z_3 are the reflection coefficients given by eqn. (1.15).

Solving eqn. (2.2), the following relations for the reflection coefficients are obtained :

$$\left.\begin{aligned} Z_1 &= \left[\sin(\theta_1 + \theta_3) + \sin(\theta_4 - \theta_3) - \frac{K_3}{K_4}\frac{R_2}{R_1}\sin(\theta_1 + \theta_4) \right]\frac{1}{\Delta}, \\ Z_2 &= [\cos(\theta_2 - \theta_3) - \cos(\theta_1 - \theta_2)]\frac{K_1}{K_3}\frac{1}{\Delta}, \\ Z_3 &= \left[\frac{K_1 K_3}{K_4^2}\frac{R_2}{R_1}\cos(\theta_1 + \theta_2) - \frac{K_1}{K_4}\cos(\theta_2 - \theta_3) \right]\frac{1}{\Delta}, \end{aligned}\right\} \quad \ldots (2.3)$$

where

$$\Delta = \frac{K_1}{K_4}\cos(\theta_2 - \theta_3) - \frac{K_1 K_3}{K_4}\frac{R_2}{R_1}\cos(\theta_2 - \theta_4). \quad \ldots (2.4)$$

3. Reflection of Longitudinal Micro-Rotation Wave from a Fixed Surface

In the present case, we study the reflection of a plane longitudinal micro-rotational wave at a fixed surface. To satisfy the boundary conditions at $z = 0$, an incident longitudinal microrotational wave travelling with speed V_2 in the direction $\vec{v_1}$ making an angle θ_1 with the plane boundary give rise to :

(I) a reflected longitudinal micro-rotation wave travelling with speed V_2 in the direction $\vec{v_2}$ and making an angle θ_2 with fixed surface,

(II) a set of reflected coupled waves travelling with speed V_3 in the direction $\vec{v_3}$ and making an angle θ_3 with the surface,

(III) a similar set of reflected coupled waves travelling with speed V_4 in the direction $\vec{v_4}$ and making an angle θ_4 with the surface.

The geometry of the problem is shown in Fig. 3.

For this case, we have

$$\vec{u} = (u_1, 0, 0), \quad \vec{\phi} = (0, \phi_2, \phi_3). \quad \ldots (3.1)$$

With the help of eqns. (1.3) and (3.1), we obtain

$$u_1 = \frac{\partial U_z}{\partial y} - \frac{\partial U_y}{\partial z}, \quad \phi_2 = \frac{\partial \xi}{\partial y} + \frac{\partial \Phi_x}{\partial z}, \quad \phi_3 = \frac{\partial \xi}{\partial z} - \frac{\partial \Phi_x}{\partial y} \quad \ldots (3.2)$$

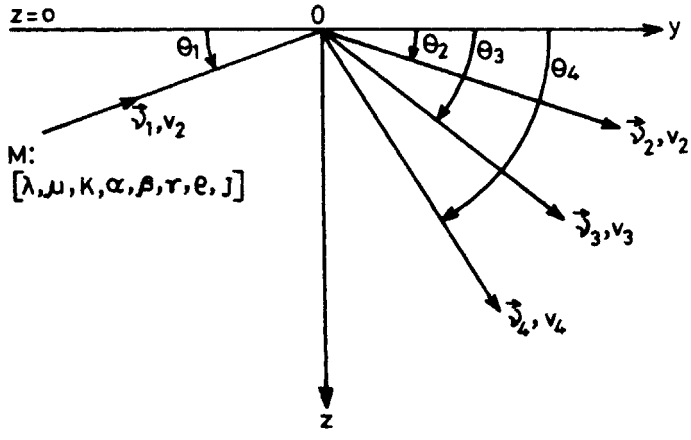

FIG. 3. Reflection of longitudinal micro-rotation wave.

The appropriate potentials are given by Parfitt and Eringen[5],

$$\left.\begin{aligned}
\xi &= b_1 \exp\left[iK_2(\cos\theta_1\, y - \sin\theta_1\, z) - i\omega_2 t\right] \\
&\quad + b_2 \exp\left[iK_2(\cos\theta_2\, y + \sin\theta_2\, z) - i\omega_2 t\right], \\
\vec{U_p} &= \left[A_{py}\vec{J} - \left(\frac{\cos\theta_p}{\sin\theta_p}\right)A_{py}\vec{K}\right]\exp\left[iK_p(\cos\theta_p y + \sin\theta_p z) - i\omega_p t\right], \\
\vec{\Phi_p} &= \vec{I}\left(\frac{\beta_{AP}}{\beta_{BP}}\right)\left(\frac{A_{py}}{\sin\theta_p}\right)\exp\left[iK_p(\cos\theta_p\, y + \sin\theta_p\, z) - i\omega_p t\right]
\end{aligned}\right\} \quad \ldots (3.3)$$

where $p = 3, 4$; b_1, b_2 are the amplitudes of incident and reflected longitudinal micro-rotational waves respectively; and A_{py} are the amplitudes of reflected coupled waves

$$\beta_{AP} = \left[\frac{K_p\,\omega_0^2}{K_p^2\left(V_4^2 - 2\dfrac{\omega_0^2}{K_p^2} - c_4^2\right)}\right]\beta_{BP}.$$

The boundary conditions are :

$$u_1 = 0, \quad \phi_2 = 0, \quad \phi_3 = 0 \quad \text{at } z = 0. \qquad \ldots (3.4)$$

Substituting the values of potentials given by (3.3) in the boundary conditions (3.4) and making use of eqns. (3.2), (1.8), (1.9), (1.12) and (1.13), we obtain

$$\left.\begin{aligned}
&(\sin\theta_4)\,Z_2 + (\sin\theta_3)\,Z_3 = 0,\\
&(\cos\theta_2)\,Z_1 + \left(\frac{\beta_{A3}}{\beta_{B3}}\right)\frac{Z_2}{K_2} + \left(\frac{\beta_{A4}}{\beta_{B4}}\right)\frac{Z_3}{K_2} = -\cos\theta_1\,,\\
&(\sin\theta_2)\,Z_1 - \left(\frac{\cos\theta_3}{\sin\theta_3}\right)\frac{\beta_{A3}}{\beta_{B3}}\frac{Z_2}{K_2} - \left(\frac{\cos\theta_4}{\sin\theta_4}\right)\left(\frac{\beta_{A4}}{\beta_{B4}}\right)\frac{Z_3}{K_2} = \sin\theta_1
\end{aligned}\right\} \quad \ldots (3.5)$$

where

$$Z_1 = b_2/b_1\,, \quad Z_2 = \frac{iK_3A_{3y}}{b_1}\,, \quad Z_3 = \frac{iK_4A_{4y}}{b_1}\,. \qquad \ldots (3.6)$$

Solving eqns. (3.5), we obtain the following relations for the reflection coefficients

$$\left.\begin{aligned}
Z_1 &= \left[\frac{\beta_{A3}}{\beta_{B3}}\frac{1}{K_2}\cos(\theta_1+\theta_3) - \frac{\beta_{A4}}{\beta_{B4}}\frac{1}{K_2}\frac{\sin\theta_1}{\sin\theta_4}\cos(\theta_1+\theta_4)\right]\frac{1}{\Delta}\,,\\
Z_2 &= \sin\theta_1\sin(\theta_1-\theta_2)\frac{1}{\Delta}\,,\\
Z_3 &= -\sin\theta_1\sin(\theta_1+\theta_2)\frac{1}{\Delta}\,,
\end{aligned}\right\} \quad \ldots (3.7)$$

where

$$\Delta = \frac{\beta_{A4}}{\beta_{B4}}\frac{1}{K_2}\frac{\sin\theta_1}{\sin\theta_4}\cos(\theta_2-\theta_4) - \frac{\beta_{A3}}{\beta_{B3}}\frac{1}{K_2}\cos(\theta_2-\theta_3). \qquad \ldots (3.8)$$

4. Numerical Results and Discussion

To study the behaviour of various reflected and refracted waves at the interface, we have calculated the modulus of amplitude ratios for various reflected and refracted waves for two models. The values of relevant elastic parameters are given below :

Model I : Following Gaüther[4], for a micropolar elastic solid half-space (Medium M_2), we have

$$\lambda = 7.54 \times 10^{11} \text{ dyne/cm}^2, \qquad \mu = 1.89 \times 10^{11} \text{ dyne/cm}^2,$$

$$K = 0.0149 \times 10^{11} \text{ dyne/cm}^2, \qquad \frac{\gamma}{\mu j} = 7.11,$$

$$\rho = 2.190 \text{ gm/cm}^3, \qquad \frac{\omega^2}{\omega_0^2} = 10.$$

For liquid half-space (Medium M_1)

$$\lambda' = 0.214 \times 10^{11} \text{ dyne/cm}^2, \qquad \rho' = 1.0 \text{ gm/cm}^3.$$

Model II : For (Medium M_2), we take

$$\lambda = 2.2 \times 10^{11} \text{ dyne/cm}^2, \qquad \mu = 1.1 \times 10^{11} \text{ dyne/cm}^2,$$

$$K = 0.088 \times 10^{11} \text{ dyne/cm}^2, \qquad \frac{\gamma}{\mu j} = 3.03,$$

$$\rho = 2.6 \text{ gm/cm}^2, \qquad \frac{\omega^2}{\omega_0^2} = 10$$

and for Medium (M_1) liquid half-space as given above.

When coupled wave is incident at solid-liquid interface, the variation of modulus of amplitude ratios of different reflected and refracted waves is different for different angle of emergence of the waves. It has been observed that these amplitude ratios become complex for a definite range of angle of emergence; for Model I, when angle of emergence is 0° to 70°; and for Model II, the range is 0° to 59°. It is so because the following quantities occurring in the elements of matrix P,

$$(1 - V_r \cos^2 \theta_1)^{1/2}, \quad (1 - V_s \cos^2 \theta_1)^{1/2}, \quad (1 - V_m \cos^2 \theta_1)^{1/2},$$

become negative.

We have calculated the modulus of amplitude ratios for those angles of emergence of waves for which these are real.

Figures 4 and 5 exhibit the behaviour of modulus of amplitude ratios w.r.t. the angle of emergence for Models I and II respectively.

The variations of modulus of amplitude ratios w.r.t. the frequency ratio ω^2/ω_0^2 greater than its critical values have also been computed numerically for these models and have been shown graphically in Figs. 6, 7 and 8. We perceive that the modulus

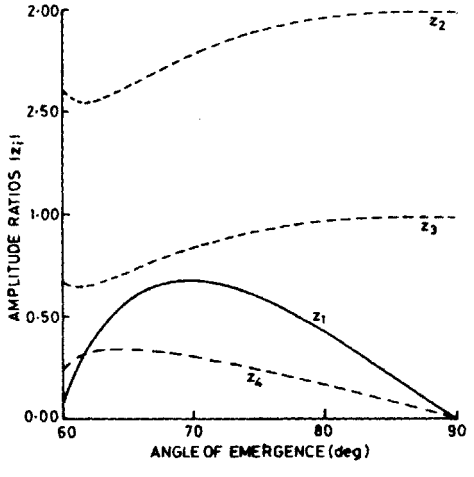

FIG. 4. Amplitude ratios $|Z_i|$ (i = 1, ..., 4) versus angle of emergence (in degrees).

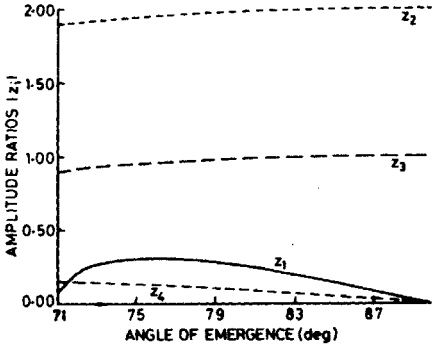

FIG. 5. Amplitude ratios $|Z_i|$ (i = 1, ..., 4) versus angle of emergence (in degrees).

of amplitude ratios increases monotonically as the frequency ratio ω^2/ω_0^2 increases for the value 2.1 to onwards and it goes to infinity for higher value of ω^2/ω_0^2.

To study the behaviour of modulus of amplitude ratios w.r.t. the angle of emergence when coupled wave is incident on the fixed boundary. We did it for Model I and the variations have been shown in Fig. 9. Also the modulus amplitude ratios w.r.t. the frequency ratio $\omega^2/\omega_0^2 > 2.0$ have been shown graphically in Fig. 10.

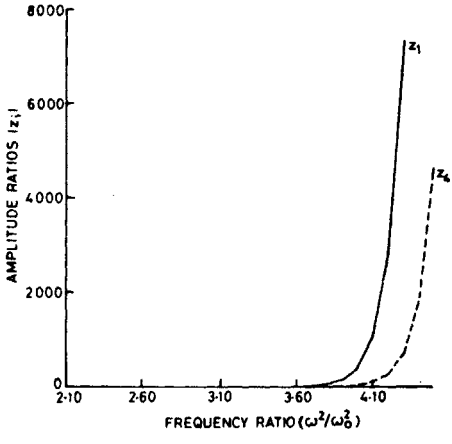

FIG. 6. Amplitude ratios $|Z_i|$ (i = 1, 4) versus frequency ratio.

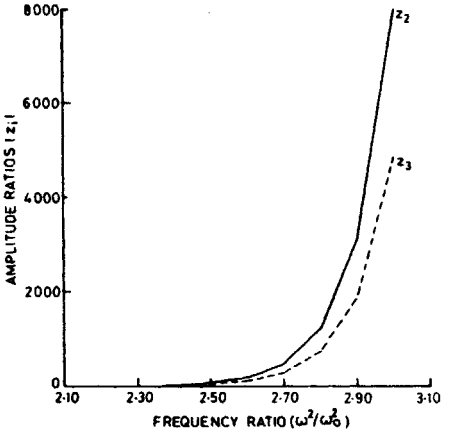

FIG. 7. Amplitude ratios $|Z_i|$ (i = 2, 3) versus frequency ratio.

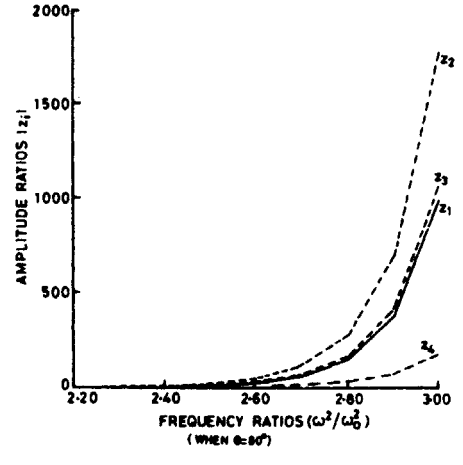

FIG. 8. Amplitude ratios $|Z_i|$ (i = 1, ..., 4) versus frequency ratio (when θ = 80°).

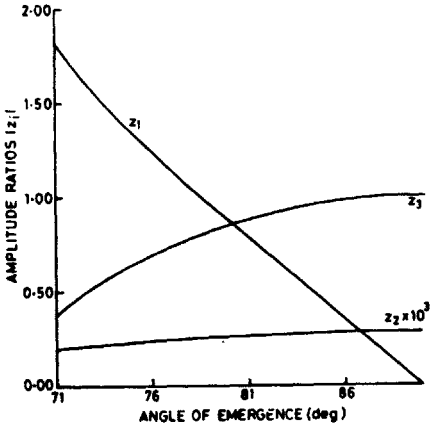

FIG. 9. Amplitude ratios $|Z_i|$ (i = 1, 2, 3) versus angle of emergence (in Degrees).

We have also computed the modulus of amplitude ratios w.r.t. angle of emergence and the frequency ratio ω^2/ω_0^2 greater than its critical values, when longitudinal micrio-rotation wave is incident on the fixed boundary for the Model I. The results are depicted in Figs. 11 and 12.

From the above, it appears that the behaviour of amplitude ratios w.r.t. frequency ratio is almost same and increases monotonically for two different model while there is a change in the behaviour of modulus of amplitude ratios w.r.t. the angle of emergence for all the three different problems.

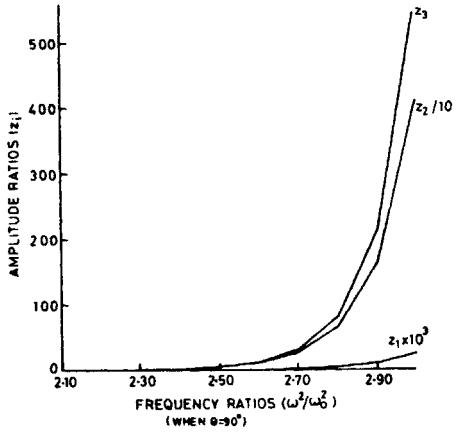

FIG. 10. Amplitude ratios $|Z_i|$ (i = 1, 2, 3) versus frequency ratio (when $\theta = 90^0$).

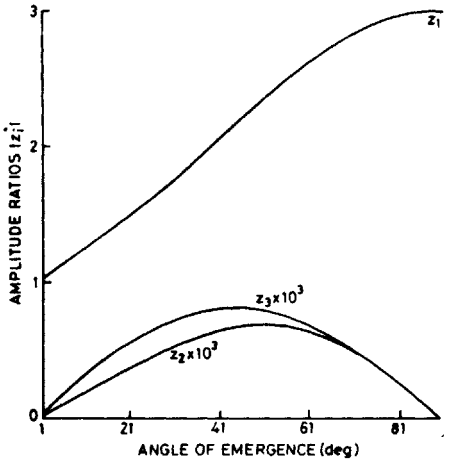

FIG. 11. Amplitude ratios $|Z_i|$ (i = 1, 2, 3) versus angle of emergence (in degrees).

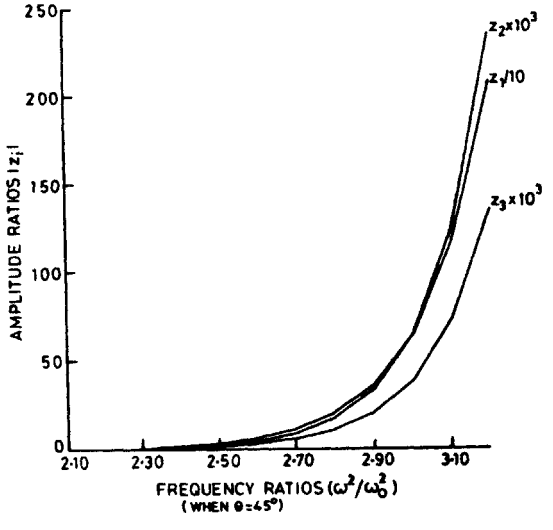

FIG. 12. Amplitude ratios $|Z_i|$ (i = 1, 2, 3) versus frequency ratio (when $\theta = 45^0$).

REFERENCES

1. A. C. Eringen and E. S. Suhubi, *Int. J. Engng. Sci.* **2** (1964), 189-203, 389-404.
2. A. C. Eringen, *J. Math. Mech.* **15** (1966), 909-24.
3. T. Ariman, *Acta Mechanica* **13** (1972), 11-20.
4. R. D. Gaüthie, *Mechanics of Micropolar Media* (eds. : O. Brulin and R. K. T. Hsieh), World Scientific Publishing Co. Pvt. Ltd., Singapore 1982, p. 459.
5. V. R. Parfitt and A. C. Eringen, *J. Acoust. Soc. Am.* **45** (1969), 1258-72.
6. S. K. Tomar and M. L. Gogna, *Int. J. Engng. Sci.* **30** (1992), 1637-46.